Mirror Design for an Omnidirectional Camera with a Space Variant Imager

Stefan Gächter, Tomáš Pajdla and Branislav Mičušík

Center for Machine Perception
Czech Technical University in Prague
Karlovo nám. 13, 121 35 Praha, Czech Republic
stefan.gachter@ieee.org
{pajdla, micusb1}@cmp.felk.cvut.cz

Abstract

Omnidirectional catadioptric cameras combine curved mirrors with conventional cameras in order to obtain a large field of view. Since the mapping from space to images becomes highly non-linear a problem of sufficiently uniform sampling of the view field appears. With a standard camera, often, a uniform rectangular sampling of the imager is transformed into a non-uniform sampling of the view field. In this paper we design the shape of the mirror that can be combined with an existing space variant imager so that a uniform sampling of the view field is obtained. We verify designed shape of the mirror with the real log-polar SVAVISCA sensor. We investigate experimentally how uniform the resolution of a resulting real uniform-resolution sensor is and compare it with the simulation.

1. Introduction

This[1] paper describes the design and experimental validation of a specific omnidirectional camera. An omnidirectional camera is a combination of a conventional camera and an axially symmetric mirror. Our goal is to design the mirror shape that matches the log-polar SVAVISCA sensor [10, 4] such that a uniform sampling of a scene around the panoramic camera is obtained. The advantage of using a polar sensor is that panoramic images are obtained directly by reading pixels out from the sensor without any additional image warping.

In the past, various mirror shapes had been presented. For this paper, the important shapes are those derived by Conroy and Moore in [3] and by Hicks and Bajcsy in [6, 7]. The mirror designed by Conroy and Moore is resolution invariant from space to image, or equivalently, achieves a constant relationship between the pixel density of the imager and the solid angle of the view field. The resultant panoramic images thus sample the scene around the camera uniformly. The mirror designed by Hicks and Bajcsy samples uniformly a plane in the scene, which is parallel to the imager plane. Their panoramic camera can be used, e.g., to observe the floor around a mobile robot. The mapping realized by their sensor maps plane to plane and therefore it is natural to have a rectangular arrangement of pixels on the imager to uniformly cover the floor around the robot.

It is also possible to use a space variant imager, which has pixels arranged in concentric rings with the same number of pixels per ring and with pixel size varying as a function of the radius. Instead of adapting the pixel sizes for a given mirror shape to equalize the image resolution, as discussed by Bruckstein and Richardson in [1], an existing imager can be used in combination with an adapted mirror shape. Chahl and Srinivasan proposed in [2] to use an imager with a log-polar pixel distribution as designed by Tistarelli and Sandini [11]. By that, a catadioptric sensor that samples uniformly a cylinder around the camera is obtained.

The contribution of this paper is the design of a mirror that matches the geometry of pixel distribution of an existing log-polar imager such that a uniform sampling of the scene is obtained. The uniformity of the sampling in azimuth is provided automatically by using the imager with a polar arrangement of pixels. On the other hand, the uniformity of the sampling along z (vertical) axis can only be achieved by designing the mirror shape to match the radial distribution of the pixels on the imager. In this paper, we designed the shape for the SVAVISCA imager but the methodology

[1]This research was supported by EU 5FP OMNIVIEWS No. 1999-29017, by the Grant Agency of the Czech Republic under the Project GACR 102/01/0971, and by the Czech Ministry of Education under Research Programme MSM 212300013.

of the design is clearly applicable for other pixel arrangements as well.

The paper is organized as follows. First, requirements for omnidirectional cameras are described in Section 2.1. The design in Section 2.2 treats first the problem of cylindrical projection without concerning the imager. Then, the solution for a non-uniform pixel density is presented. The theory is verified by experiments in Section 3. Both simulations Section 3.1 as well as the measurements on the real mirror and SVAVISCA sensor are presented, Section 3.2. Conclusions are given in Section 4.

2. Mirror shape design

2.1. Requirements

It is advantageous to use an omnidirectional camera to detect and track moving objects. This task is simplified when the size of the object as projected into the images does not depend on the position of the object in the image. If the aim of a system is to detect and track moving objects, e.g. human faces, it is suitable to have an omnidirectional camera providing images with the size of the object forefront depending only on the distance of the object from the camera. If only small objects are assumed the forefronts of objects at the same distance from the axis of a catadioptric camera lie approximately on a cylinder, see Figure 1. Therefore, the catadioptric sensor has to project the cylinder to the image such that its geometry is preserved. Thanks to the axial symmetry, the problem is restricted to ρz-plane and the mirror shape has to be designed such that at a given distance d from the origin the vertical dimension h is linearly mapped to the radial distance from the center of the image plane ρ, as shown in Figure 2.

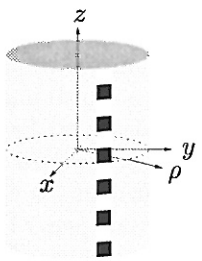

Figure 1: Cylinder surface for which an object forefront has to preserve its geometry.

2.2. Mirror shape derivation

The relationship between a world point with coordinates $[d\ h]^T$, the cross section function $F(t)$ with $t(\rho)$, and an image point with coordinates $[\rho\ 0]^T$ is defined by the law of reflection, see Figure 2 and Figure 4. Instead of deriving directly $F(t)$, an expression for $h(t)$ is found. This is not the most obvious way to find the cross section function but it results in some useful equations for the simulation of the sensor.

Referring to Figure 2, the height $h(t)$ of the world point at a distance d is given as

$$h(t) = F(t) - \cot(\phi)(d - t)\ , \tag{1}$$

where t is a function of ϱ as shown on Figure 4. This means that the ray emanating from an image point is reflected by the mirror and reaches the world point on the cylinder. The incident and coincident rays on the mirror, depicted in Figure 3, are described by their directional vectors $\vec{i}$ and $\vec{c}$ respectively. Both vectors have norm equal one. The law of reflection imposes that the angle between the incident ray and the normal to the surface is equal to the angle between the normal and the coincident ray. The normal vector $\vec{n}$ corresponds to a function of derivatives of the cross section function $F(t)$ at the point t. Expressed by the scalar product, the following condition must hold

$$-\vec{i} \cdot \vec{n} = \vec{n} \cdot \vec{c}\ . \tag{2}$$

The components of the vectors are as follows

$$\vec{i} = \frac{\vec{r}}{|\vec{r}|} = \begin{bmatrix} i_\rho \\ i_z \end{bmatrix}\ , \quad \vec{r} = \begin{bmatrix} t \\ F(t) - f \end{bmatrix}\ ,$$

$$\vec{n} = \begin{bmatrix} \mathrm{d}F(t) \\ -\mathrm{d}t \end{bmatrix}\ , \qquad \vec{c} = \begin{bmatrix} c_\rho \\ c_z \end{bmatrix}\ .$$

Looking at (1), the term $\cot(\phi)$ has to be expressed as a function of the given geometry. The law of reflection imposes $2\gamma + \theta + \phi = \pi$ and therefore the slope of the coincident ray is given by $\frac{c_z}{c_\rho} = \cot(2\gamma + \theta) = -\cot(\phi)$. Since $\tan(\phi)$ corresponds to the slope $\frac{c_z}{c_\rho}$ of the coincident ray and because the slope of the incident ray can be expressed either by the vector $\vec{i}$ or $\vec{r}$, the following equation is obtained from (2)

$$\frac{c_z}{c_\rho} = F'(t) + \frac{i_\rho}{c_\rho}\left(F'(t) - \frac{F(t) - f}{t}\right). \tag{3}$$

The condition for two unity vectors, $\|\vec{i}\| = \|\vec{c}\| = 1$, gives the expression for the fraction $\frac{i_\rho}{c_\rho}$,

$$\left(\frac{i_\rho}{c_\rho}\right)^2 = \frac{1 + \left(\frac{c_z}{c_\rho}\right)^2}{1 + \left(\frac{F(t) - f}{t}\right)^2}\ . \tag{4}$$

Combining the equation (3) and (4) results in expression

$$h(t) = F(t) + \frac{2tF'(t) - (F(t) - f)(1 - F'(t)^2)}{2(F(t) - f)F'(t) + t(1 - F'(t)^2)}(d - t) \ . \tag{5}$$

Solving this equation for the derivative of the cross section function $F'(t)$ results in a cubic differential equation. The differential equation, which defines the convex mirror shape, is consequently given by the following expression

$$F'(t) + \frac{t(d-t) + (F(t) - f)(F(t) - h(t))}{(F(t) - f)(d - t) - t(F(t) - h(t))}$$

$$-\sqrt{\left(\frac{t(d-t) + (F(t) - f)(F(t) - h(t))}{(F(t) - f)(d - t) - t(F(t) - h(t))}\right)^2 + 1} = 0 \ . \tag{6}$$

Three parameters influence the mirror shape: (i) the focal length f of the camera, (ii) the distance d, which corresponds to the perimeter of the projected cylinder, and (iii) the function $h(t)$, which corresponds to the vertical dimension of the world point. The parameter $h(t)$ defines the characteristic of the catadioptric sensor. To have a linear relationship between the height h of a world point and the radius ϱ of an image point, the following condition must hold

$$h(\rho) = a \log_k \left(\frac{\rho}{\rho_0}\right) + b \ . \tag{7}$$

When substituting this expression into (6), the image coordinate ρ must be replaced by t. The relation between ρ and t results from the projection by a conventional camera

$$\rho = \frac{ft}{F(t) - f} \ . \tag{8}$$

A closed form solution for (6) combined with (7) and (8) seems not to be easily available. Therefore, we solved the problem numerically. The solution for the above differential equation is computed with the *MatLab* function `ode45.m`. This gets the best result compared with the other solvers of *MatLab* and that of *Mathematica*.

Using an imager with a log-polar pixel density, the condition has to be of the form (7), where ρ is the radius, ρ_0 the innermost circle of the log-polar layout and k the growth rate of the pixel size, see Figure 5. The pixel size is linearly increasing from the foveal region towards the periphery. The free parameter a and b are called gain and offset respectively. The foveal region of the SVAVISCA sensor does not have log-polar pixel distribution in the center up to the radius

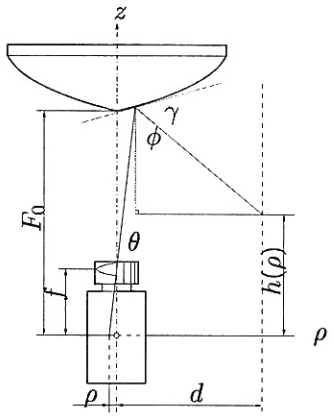

Figure 2: Schematic diagram of the catadioptric sensor.

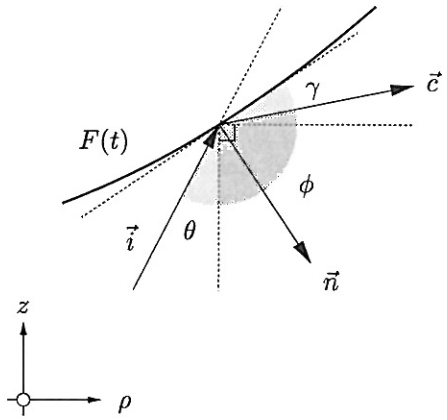

Figure 3: Reflection of a ray at the mirror surface.

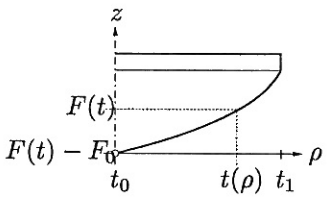

Figure 4: Cross section function.

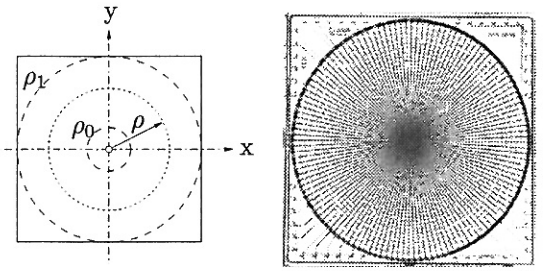

Figure 5: Pixel density of the form log-polar for the camera imager. Figure (a) depicts the geometry and figure (b) an example imager similar to the SVAVISCA (by courtesy of G.Sandini).

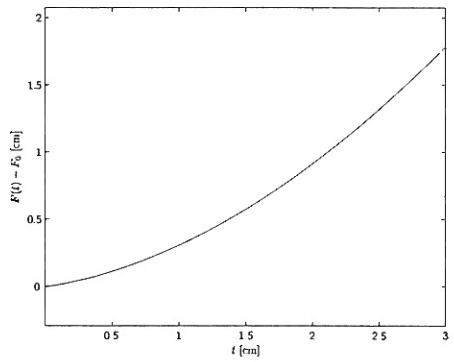

Figure 6: The cross section of the mirror function for $a = 4$ and $b = -400$ cm, gives the field of view of approximately 69.6° ($\phi_0 = 26.7°$ and $\phi_1 = 96.3°$).

$\rho_0 = 272.73\,\mu$m. However, for simplicity in the mirror design, this is neglected and the region is assumed to have a log-polar pixel distribution extrapolated from the periphery. See [8] for exact specification of the imager. The following parameters influence the mirror design: the focal length f, the radius of the mirror rim t_1, the gain a, and the offset b. For the following solution, d equals 2 m and f it is equal to 25 mm. The mirror rim parameter $t_1 = 3$ cm, the maximal imager dimension ρ_1 is 3.6 mm, and F_0 is fixed to 21.5 cm. The resulting cross section function is shown in Figure 6 and the distribution of the reflected rays in Figure 7. The technical drawing for the mirror is depicted in Figure 9(a) and a picture of the manufactured mirror is shown in Figure 9(b). The field of view is approximately 69.6° assuming that only periphery of the imager is used.
The mirror was designed for the fixed distance $d = 2m$. However, it is also interesting to see how the imaging behaves for objects outside the reference cylinder. As a criterion, the ratio between the numerical derivative of the function $h(\rho)$, $\frac{\Delta h}{\Delta \rho}$, given by (5), and its theoretical derivative $\frac{dh}{d\rho} = \frac{a}{\ln(k)} \frac{1}{\rho}$ given by (7), is computed. This ratio is normalized to the distance by dividing it with the factor $\frac{d_i}{d}$, where $d_i \in \{1\text{m}, 1.5\text{m}, 2\text{m}, 3\text{m}, 4\text{m}\}$. The result is depicted in Figure 8. The optimal ratio should be equal to one over the whole range of ρ. This is even not the case for the reference distance d. Due to the numeric solution, a systematic error exists. The mapping between the world and image dimension is only approximately linear. The deviation of the ratios from the optimal ratio, which is equal to one, is decreasing with increasing ρ, therefore the distortion in the mapping is increasing in the top-to-bottom direction. The ratios do not vary much with the distance. Therefore, the mirror realizes approximately a perspective projection.

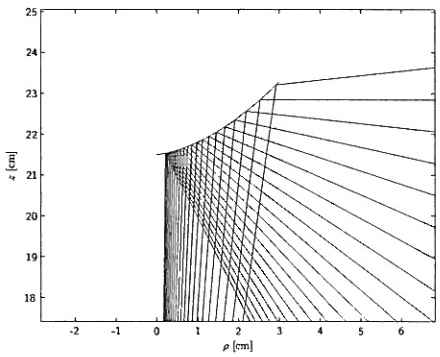

Figure 7: Rays reflected by the mirror which proportionally scale s the vertical dimension. The imager has a log-polar arrangement of pixels.

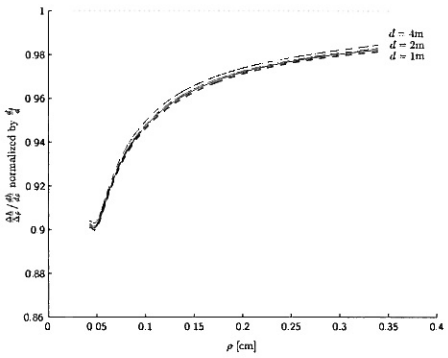

Figure 8: The ratio of the numerical derivative of the function $h(\rho)$, $\frac{\Delta h}{\Delta \rho}$, and its theoretical derivative $\frac{dh}{d\rho} = \frac{a}{\ln(k)} \frac{1}{\rho}$. The ratio is normalized to the distance by dividing it with the factor $\frac{d_i}{d}$, where $d_i \in \{1\,\text{m}, 1.5\,\text{m}, 2\,\text{m}, 3\,\text{m}, 4\,\text{m}\}$.

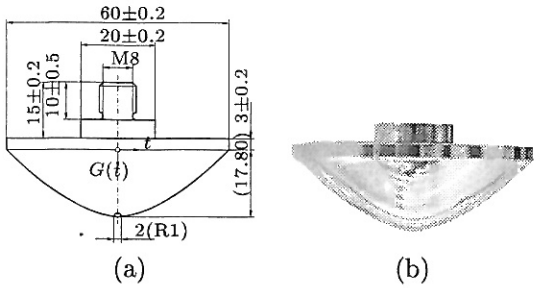

(a) (b)

Figure 9: (a) the technical drawing for the mirror matching with the non-uniform pixel density (SVAVISCA), (b) the manufactured mirror.

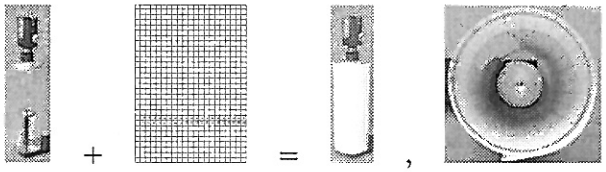

Figure 10: Acquisition of artificial scenes.

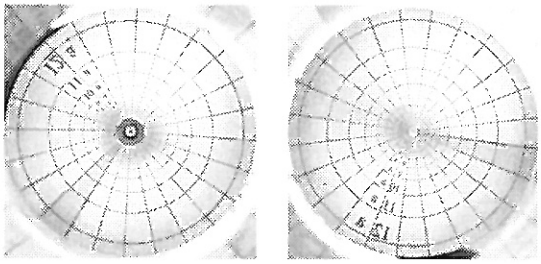

(a) (b)

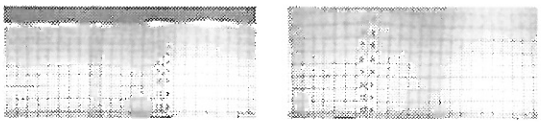

(c) (d)

Figure 11: Raw and panoramic images from various mirrors. In (a) hyperbolic mirror, in (b) a mirror for SVAVISCA uniform resolution is used. In (c) and (d) the panoramic images obtained by SVAVISCA re-sampling of (a) and (b) are depicted.

3. Experiments

3.1. Simulations

This section presents the simulated experiments with the designed mirror. The designed mirror is compared with a hyperbolic mirror that provides true central panoramic images of the scene. All images were recorded with a conventional camera and the mirrors were placed to the distance about $30cm$ from the image plane. The mirror projects an equidistant mesh wrapped around the sensor as schematically depicted in Figure 10. The diameter of the cylinder is about $15cm$. The diameter is much smaller than $2m$ for which the mirror was designed but the images show the expected characteristics. The images are simulated in that sense that a real cylinder with a real mesh and real mirrors were taken by a *normal* CCD camera with rectangular arrangement of pixels. The SVAVISCA images were obtained by re-sampling the conventional images according to the SVAVISCA pixel distribution. After SVAVISCA re-sampling, lines from the cylinder taken by a hyperbolic mirror are not equidistant. They are equidistant when the newly designed SVAVISCA mirror is used. We can see that the re-sampled image Figure 11(d) taken with the newly designed mirror shows a uniform projection of a uniform grid while the image Figure 11(c) taken with the hyperbolic mirror shows a non-uniformly distorted image of the same grid.

3.2. Real measurement

In this section we study experimentally the constancy of mapping of a real world to the imager along the y coordinate in the unwarped panoramic image. The mirror was designed such that vertical intervals of a constant length, Figure 1, should be mapped to image intervals of a constant length. It must hold true for any vertical interval in a constant distance from the camera-mirror axis independently from its height in the scene. However, due to the numeric solution of the mirror cross section function, a systematic error [5] exists. We cannot also forget the non-linearity (e.g. radial distortion) of the optics. The mapping between the world and image dimensions are therefore only approximately linear.

The parameters of the mirror were designed for distance $d = 200cm$ but we provide measurements also for other distances. SVAVISCA sensor with the log-polar pixel distribution was used. All parameters (focus length, distances) were set like in [5].

We moved the reference target along a sequence of positions in the vertical direction in a constant distance d from the camera-mirror axis. We carried out the experiment for distances $d = 10cm$, $d = 20cm$, $d = 30cm$, and $d = 200cm$. Figure 12 depicts these experiment. Figure 13 shows target and the orientation of axes in images. More details are described in [9]. Figure 14(a) shows $\Delta\rho$ as a function of ϕ. We calculated relative

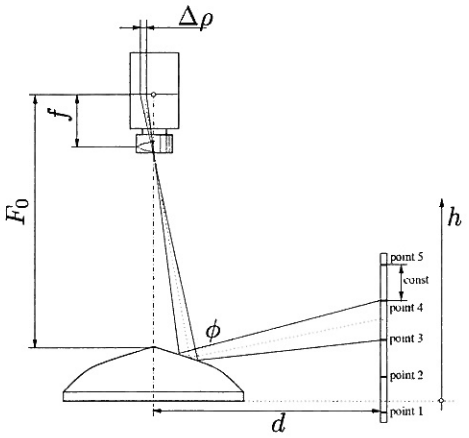

Figure 12: Schematic diagram of the experiment.

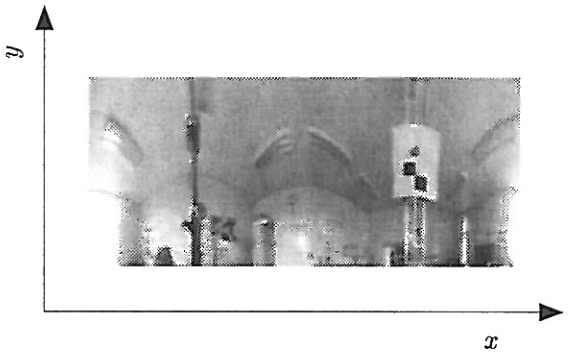

Figure 13: Axes orientation in panoramic images.

errors

$$rel.error_i = \frac{\Delta\rho_i - \Delta\rho_1}{\Delta\rho_1} 100\ [\%] \qquad (9)$$

for each step, see Figure 14(b).

Experiments show differences between theoretical design and the real mirror. The maximal deviation from the linearity depends on y-coordinate in the image and it is maximally 10% higher than what was expected from the simulations in the design phase. The error is almost independent of the distance of the target from the camera-mirror axis.

4. Conclusions

This paper has presented the design of a mirror for a catadioptric sensor. The mirror was designed such that when combined with the log-polar SVAVISCA imager, a uniform resolution panoramic image is obtained.

The mirror was designed to possess the uniform resolution property for the camera-object distance equal two meters but experiments has shown that the resolution uniformity is very similar in the distance ranging from 20 cm to two meters. The experiments has also shown that the length of the image of a fixed interval in the scene is decreasing with increasing y-coordinate in the panoramic image. From the design, it was expected that the maximal deviation from linearity would be around 10%. The real experiments has shown that the maximal deviation from linearity reached 20% almost independently of the distance from the camera.

In general, the work presented here shows that we were able to reach satisfactory results in designing uniform resolution image formation with a non-uniform imager and a convex mirror. We believe that the uniformity can still be improved by modeling other non-linearities, e.g. the radial distortion of the optics or im-

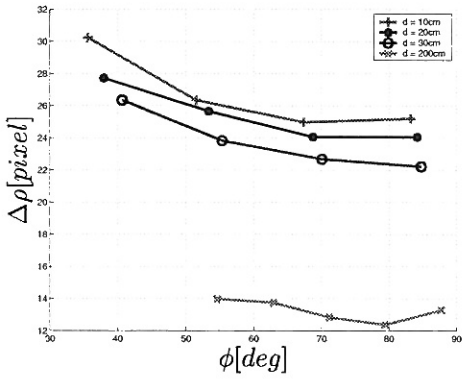

(a)

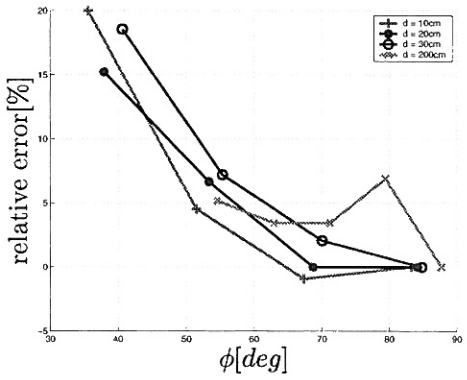

(b)

Figure 14: (a) Distances between images of each two consecutive targets as a function of angle ϕ (b) and relative error of the deviation from linearity for distances $d = 10cm$, $20cm$, $30cm$ and $200cm$ from the camera-mirror axis respectively.

proving the numerical solution of the differential equations.

References

[1] A. Bruckstein and T. Richardson. Omniview cameras with curved surface mirrors. In *IEEE Workshop on Omnidirectional Vision*, June 2000.

[2] J. Chahl and M. Srinivasan. Reflective surfaces for panoramic imaging. *Applied Optics*, 36(31):8275–85, November 1997.

[3] T. Conroy and J. Moore. Resolution invariant surfaces for panoramic vision systems. In *Proceedings of the IEEE International Conference on Computer Vision*, volume 1, pages 392–7, 1999.

[4] F. Ferrari, J. Nielsen, P. Questa, and G. Sandini. Space variant imaging. *Sensor Review*, 15(2):17–20, 1995.

[5] S. Gächter and T. Pajdla. Mirror design for an omnidirectional camera with a uniform cylindrical projection when using the SVAVISCA sensor. Technical Report CTU-CMP-2001-03, Centre for Machine Perception, Czech Technical University in Prague, 2001.

[6] A. Hicks and R. Bajcsy. Reflective surfaces as computational sensors. In *CVPR-Workshop on Perception for Mobile Agents*, June 1999.

[7] A. Hicks and R. Bajcsy. Catadioptric sensor that approximate wide-angle perspective projections. In *IEEE Workshop on Omnidirectional Vision*, June 2000.

[8] A. Mannucci, P. Questa, and D. Scheffer. D1-Document on Specification, Esprit Project N. 31951 - SVAVISCA, Version 1.0. 1999.

[9] B. Mičušík and T. Pajdla. Real uniform resolution of svavisca sensor - experimental validation. Technical Report CTU-CMP-2001-16, Centre for Machine Perception, Czech Technical University in Prague, 2001.

[10] F. Panerai, C. Capurro, and G. Sandini. Space variant vision for an active camera mount. *SPIE*, 2488, 1995.

[11] M. Tistarelli and G. Sandini. On the advantage of polar and log-polar mapping for direct estimation of time-to-impact from optical flow. *IEEE Transaction on Pattern Analysis and Machine Intelliegence*, 15(4):401–10, April 1993.